

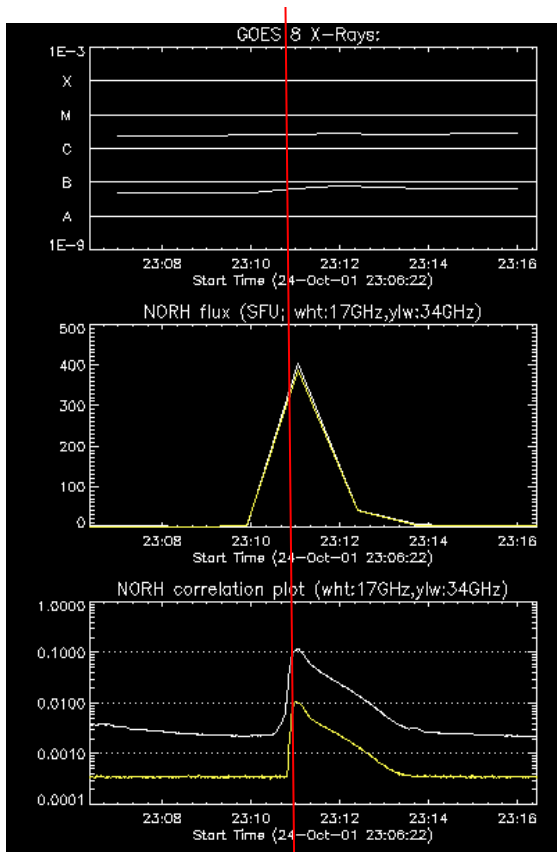
Cold Solar Flares

Gregory Fleishman, Alexandra Lysenko, Valentin
Pal'shin, Natalia Meshalkina, Larissa Kashapova,
Alexander Altyntsev

11/25/2015

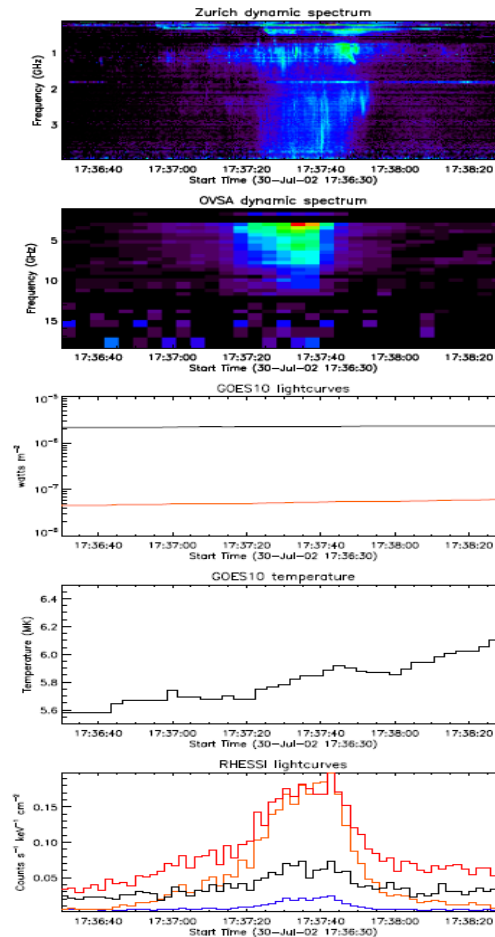
Overview of Reported CFs

Bastian et al. 2007

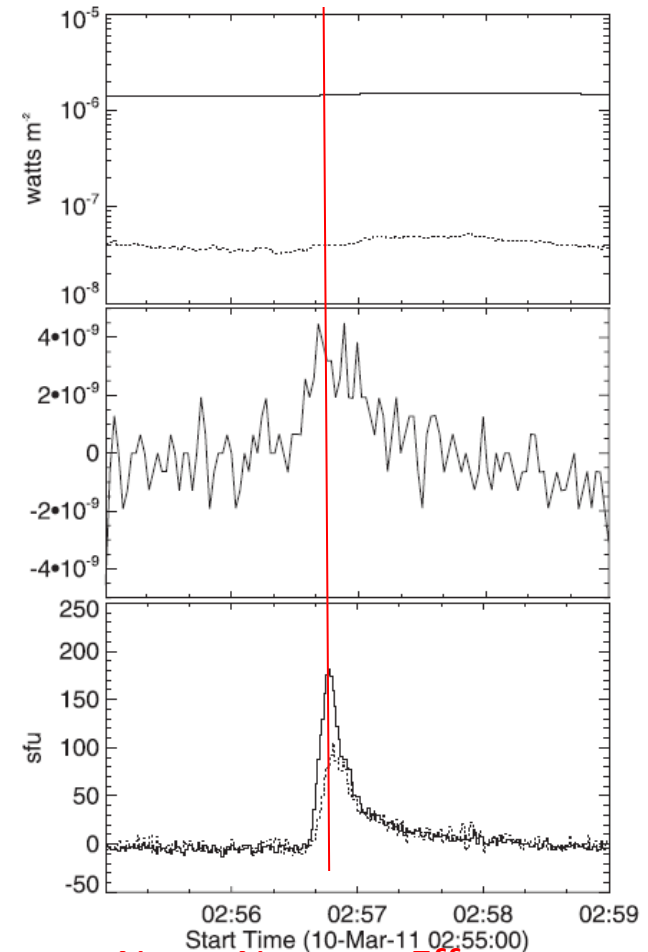


Note: Neupert Effect

Fleishman et al. 2011



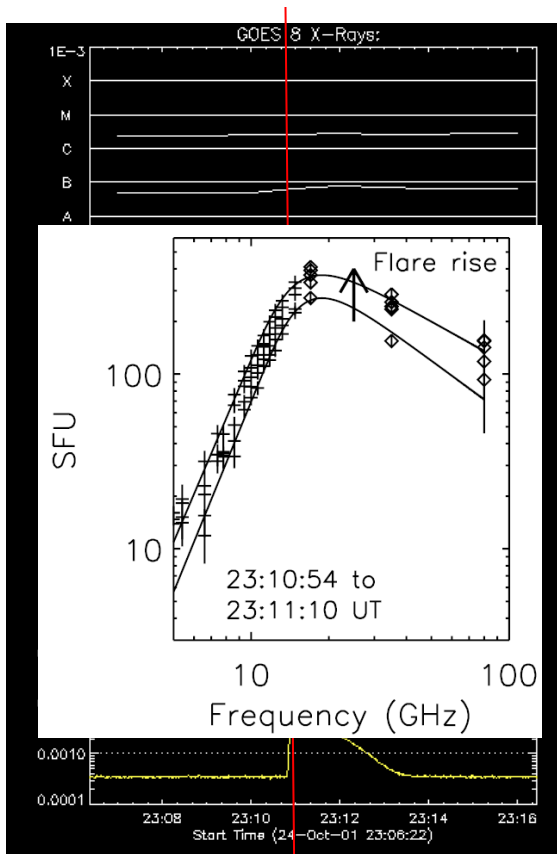
Masuda et al. 2013



Note: Neupert Effect

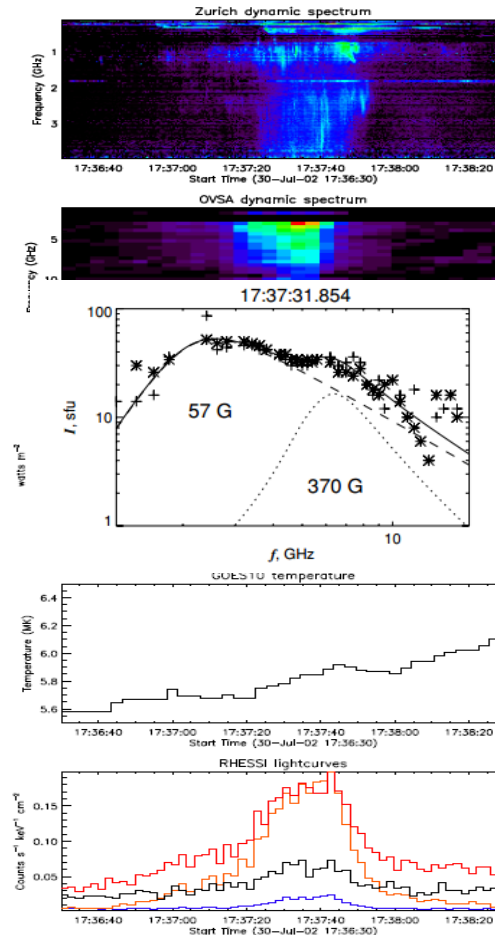
Overview of Reported CFs

Bastian et al. 2007

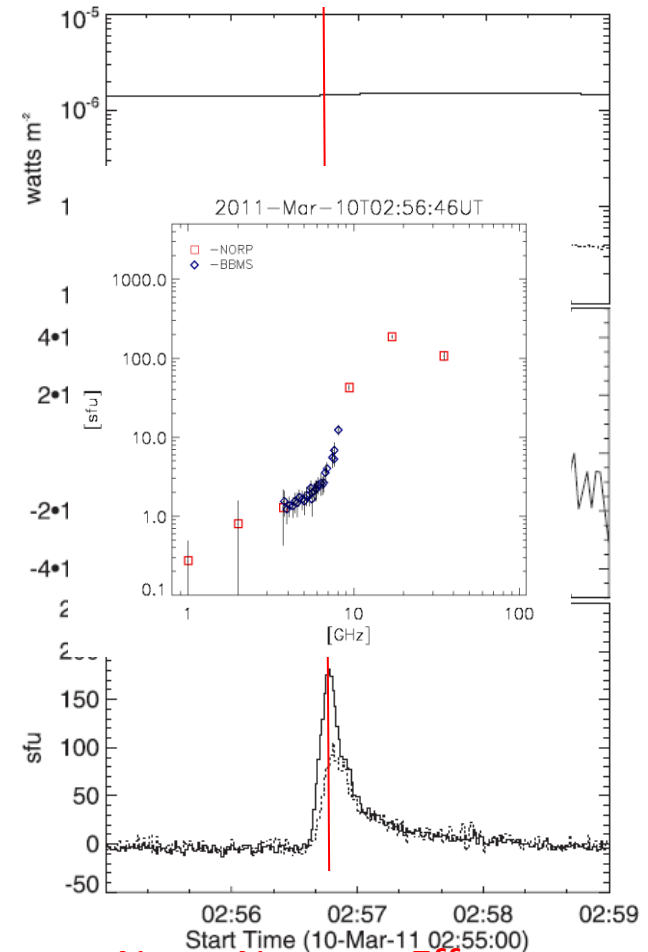


Note: Neupert Effect

Fleishman et al. 2011



Masuda et al. 2013

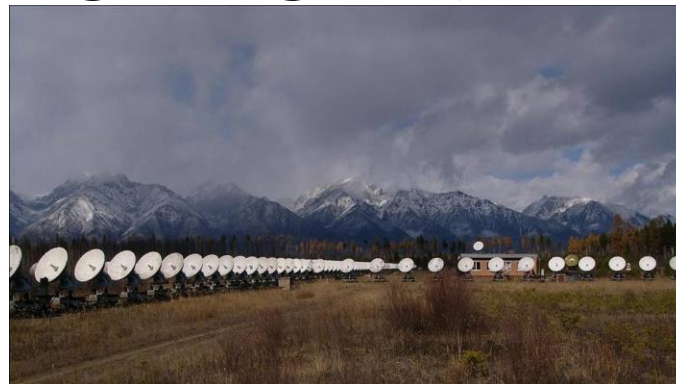
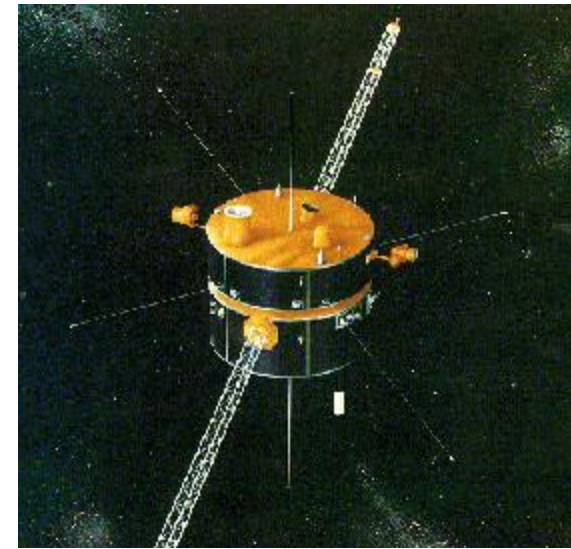


Note: Neupert Effect

Case Study: CF 2002-03-10.

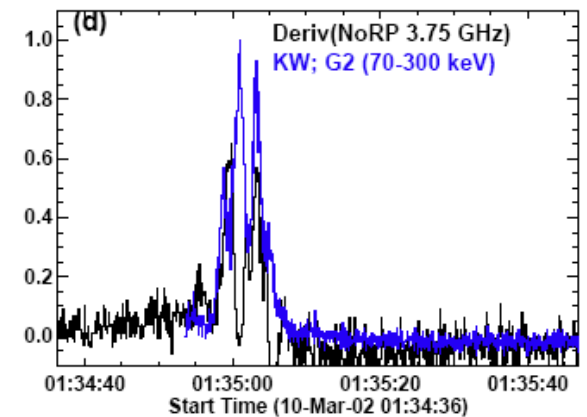
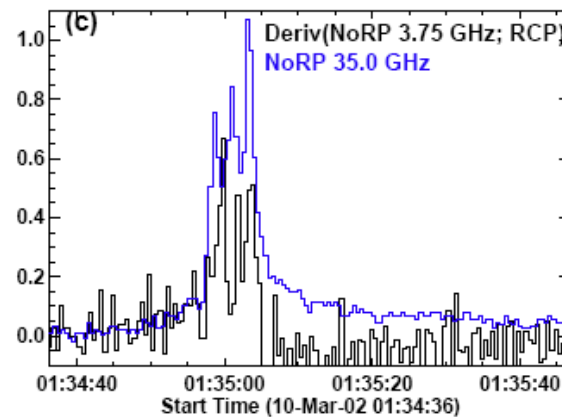
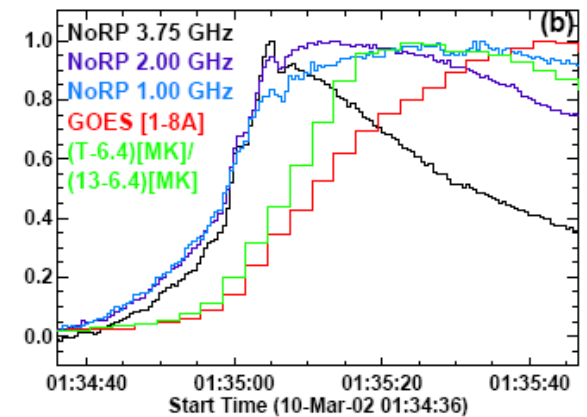
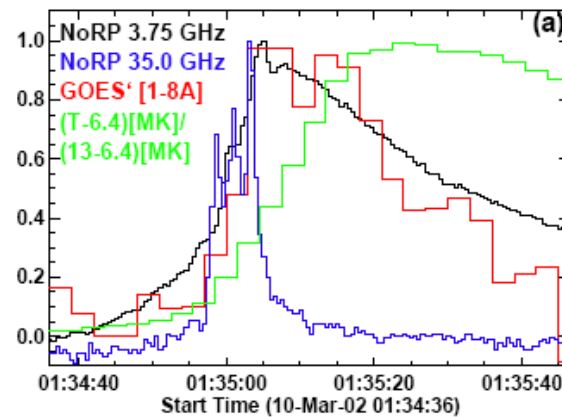
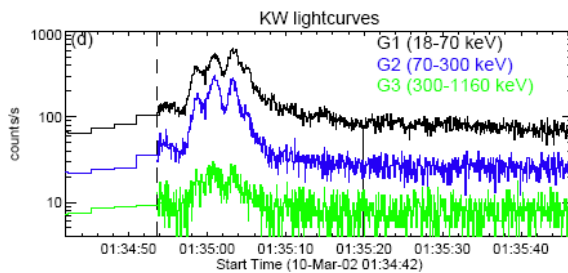
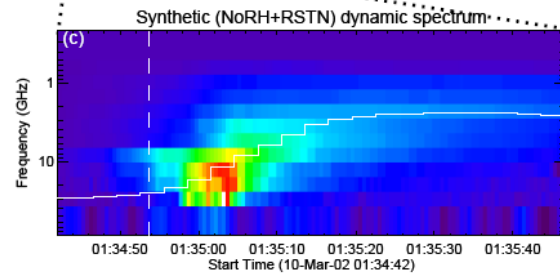
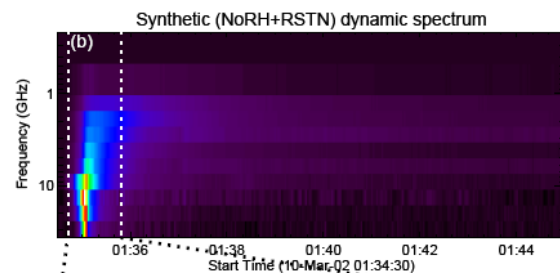
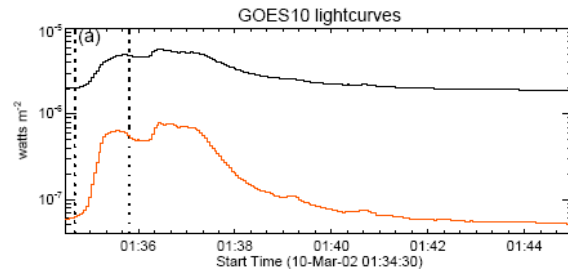
Instruments Used

- Hard X-Ray (HXR): Konus-Wind
- Soft X-Ray (SHR): GOES
- Microwave (MW): NoRH, SSRT, NoRP, RSTN
- EUV: SoHO/EIT
- Optical (LOS magnetogram): SoHO/MDI

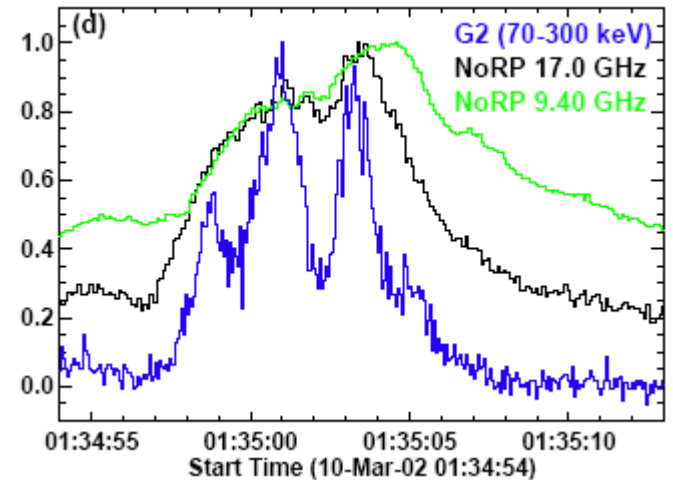
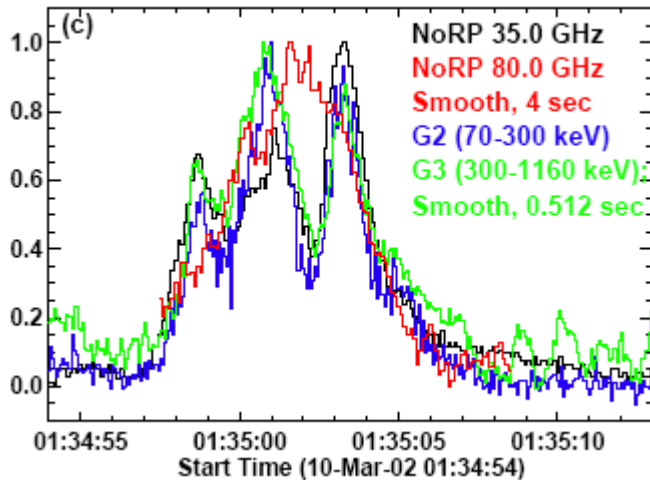
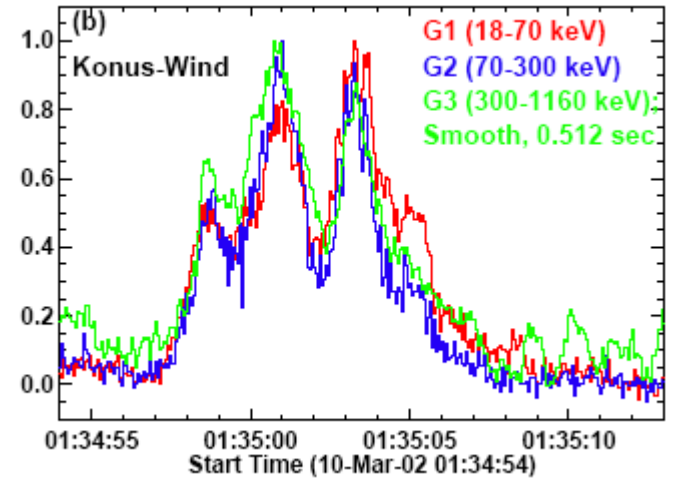
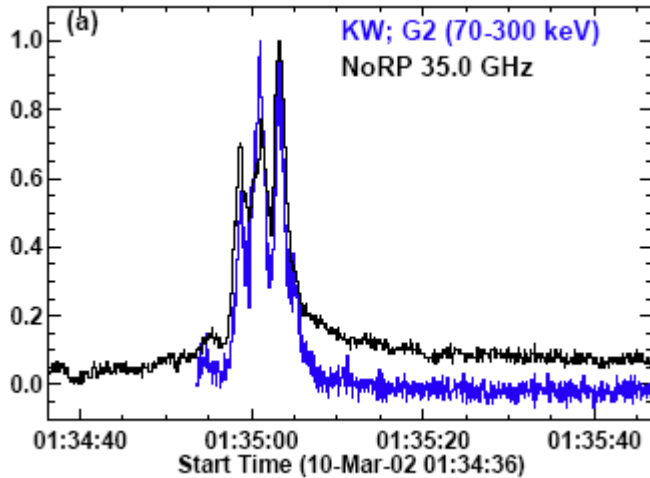


Case Study: CF 2002-03-10

GOES C5 flare – overview

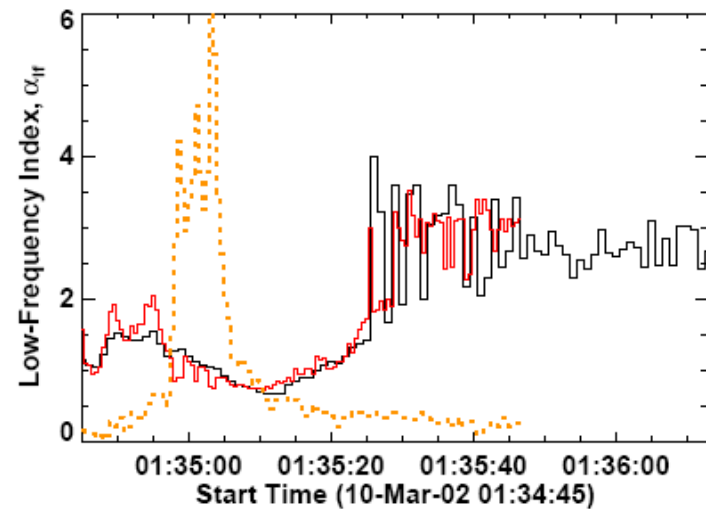
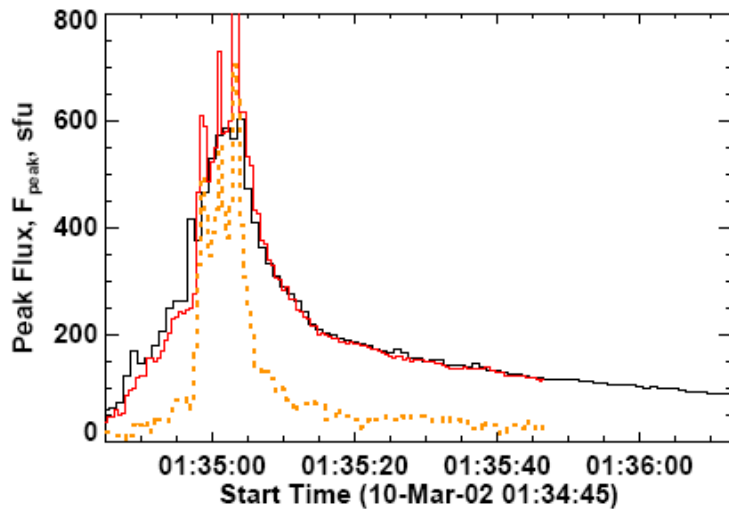
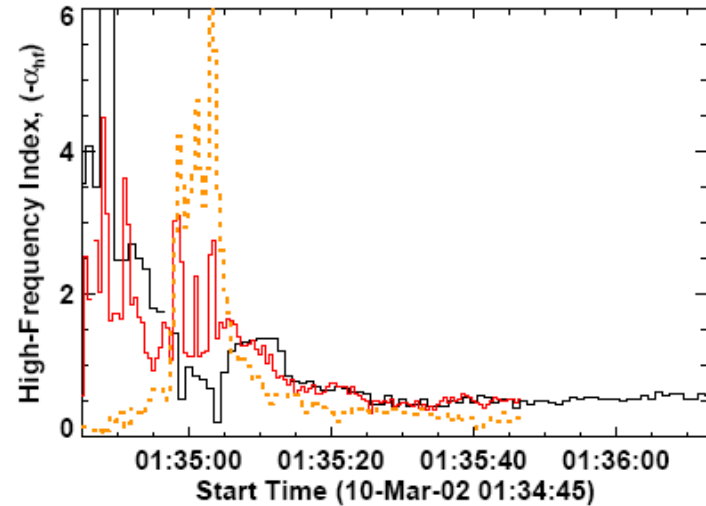
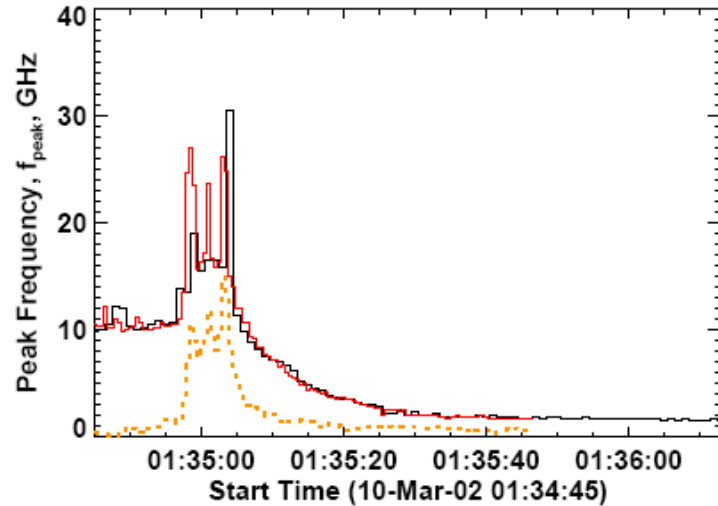


Impulsive Light Curves

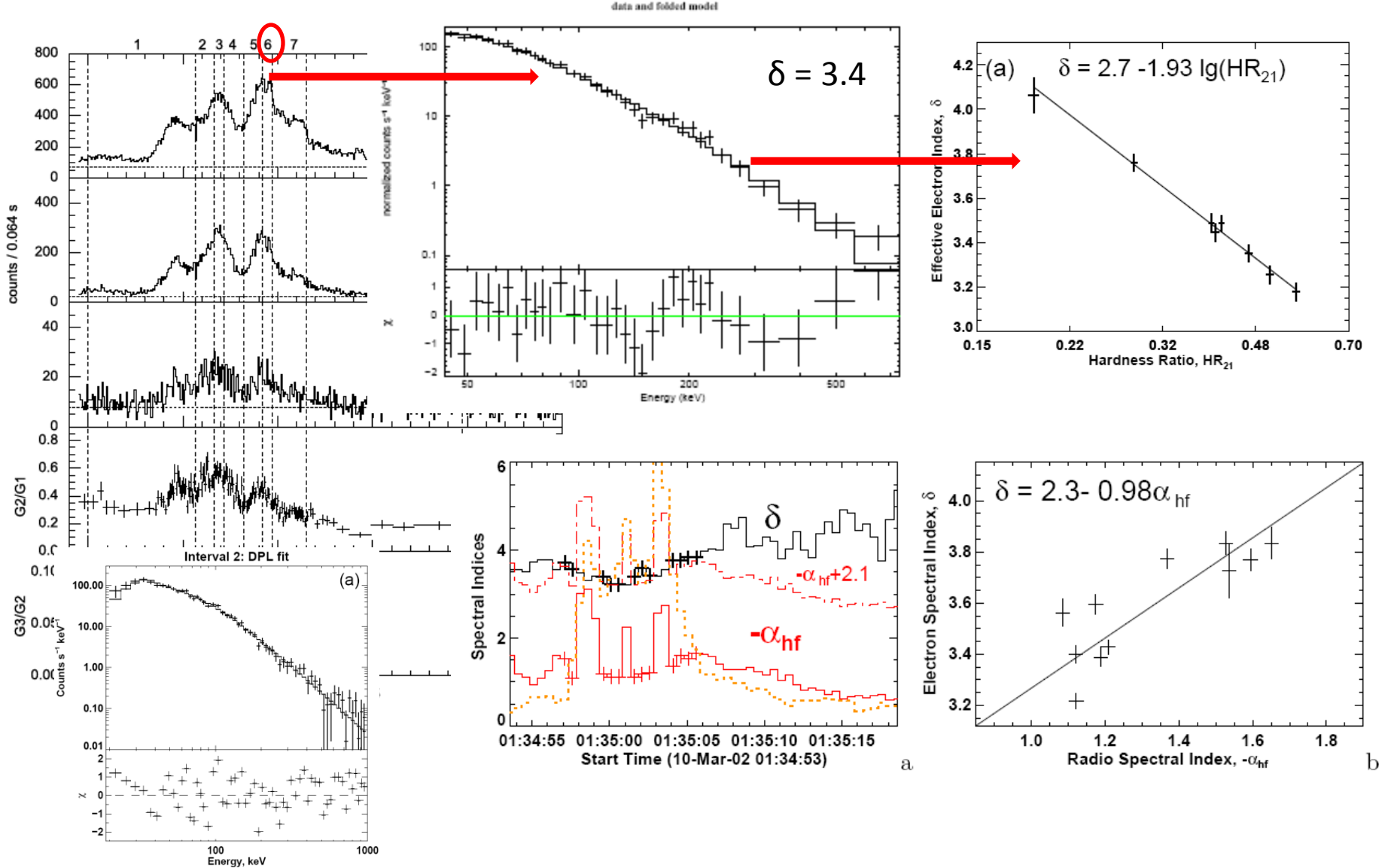


MW Fit Results

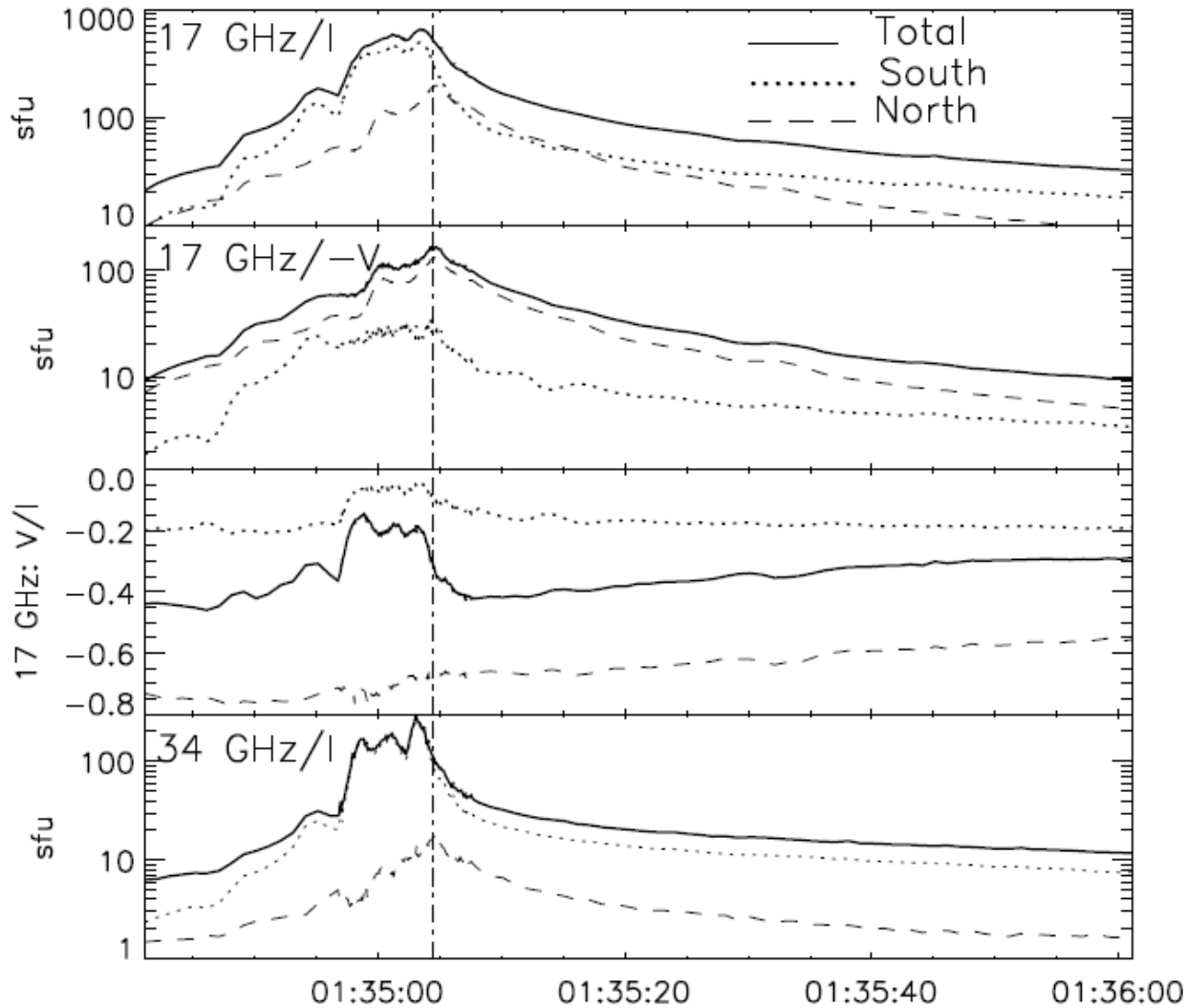
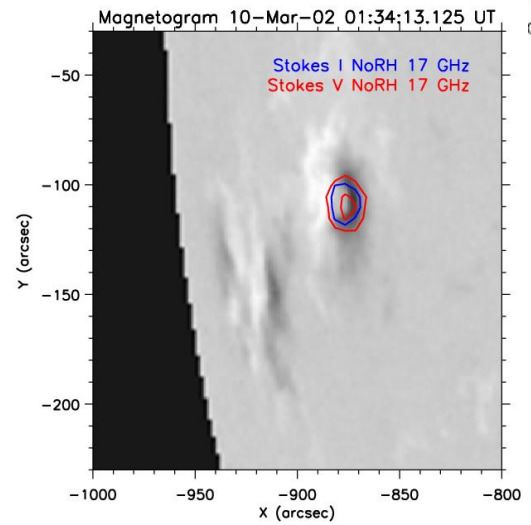
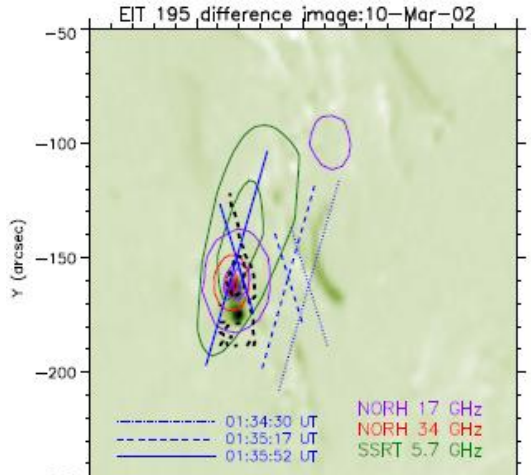
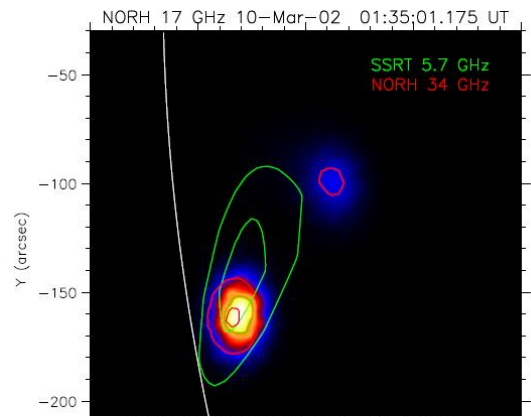
$$S = e^A f^\alpha \left[1 - e^{-e^B f^{-\beta}} \right]$$



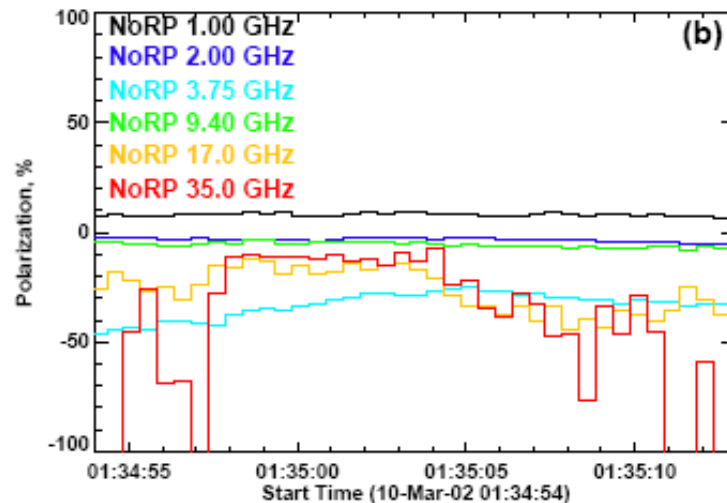
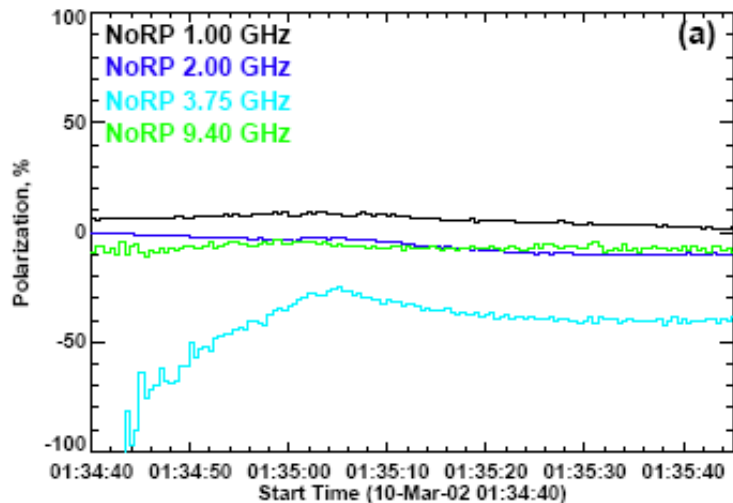
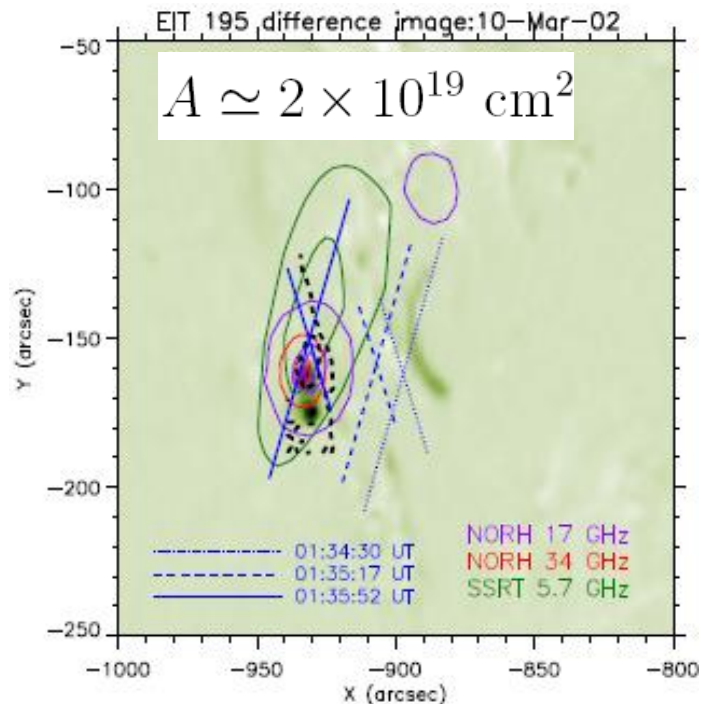
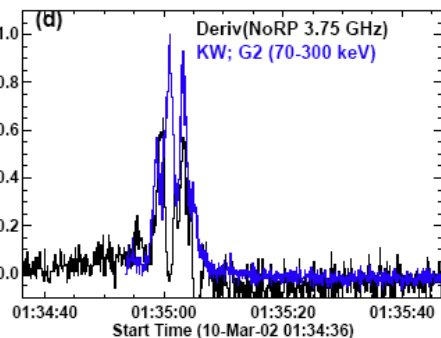
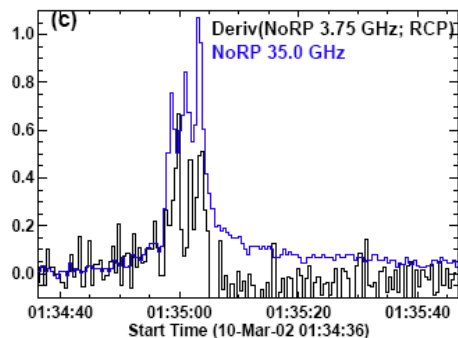
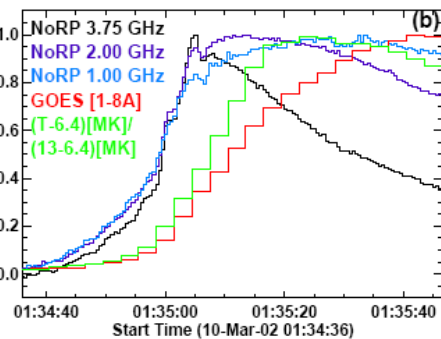
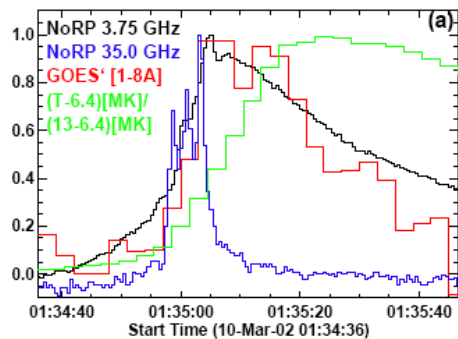
KW Fit Results (Thick-target Model; Single Power-Law with Index δ)



Images and Spatially Resolved Data



Nonthermal vs Thermal Emissions



Nonthermal vs Thermal Emissions

$$F_{\text{LCP}} \simeq F_{\text{RCP}} \simeq 6 \text{ [sfu]} \left(\frac{f}{1 \text{ GHz}} \right)^2 \left(\frac{T}{10^7 \text{ K}} \right) \left(\frac{A}{10^{20} \text{ cm}^2} \right)$$

$$\tau \simeq 2.4 \cdot 10^3 \text{ [s]} \left(\frac{L}{10^{10} \text{ cm}} \right)^2 \left(\frac{n_e}{10^{10} \text{ cm}^{-3}} \right) \left(\frac{10^7 \text{ K}}{T} \right)^{5/2}$$

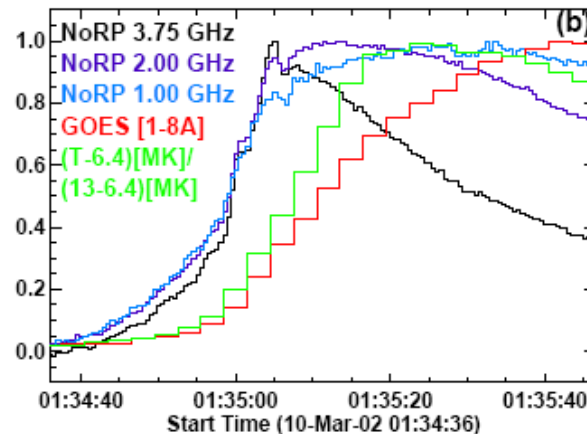
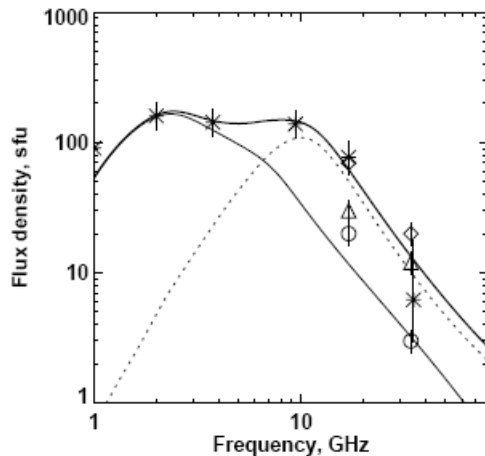
$$\tau_{5.7\text{GHz}} \sim 30 \text{ s}; \quad A \simeq 2 \times 10^{19} \text{ cm}^2$$

$$T \sim 25 \text{ MK}$$

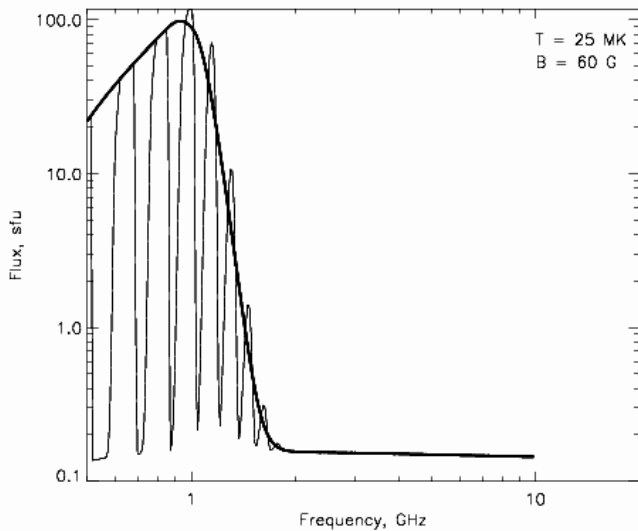
$$L \sim 10^{10} \text{ cm}$$

$$n_e \sim 10^9 \text{ cm}^{-3}$$

$$EM \sim 10^{46} \text{ cm}^{-3}$$



Nonthermal vs Thermal Emissions



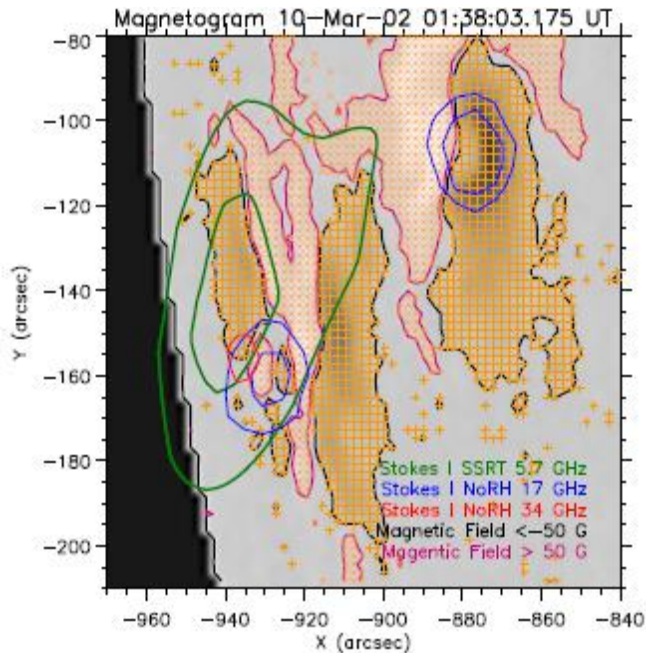
$$T \sim 25 \text{ MK}; A \sim 4 \cdot 10^{20} \text{ cm}^2$$

$$\tau_{1\text{GHz}} \sim 150 \text{ s} \quad n_e \sim 10^9 \text{ cm}^{-3}$$

$$V \sim 3 \cdot 10^{30} \text{ cm}^3$$

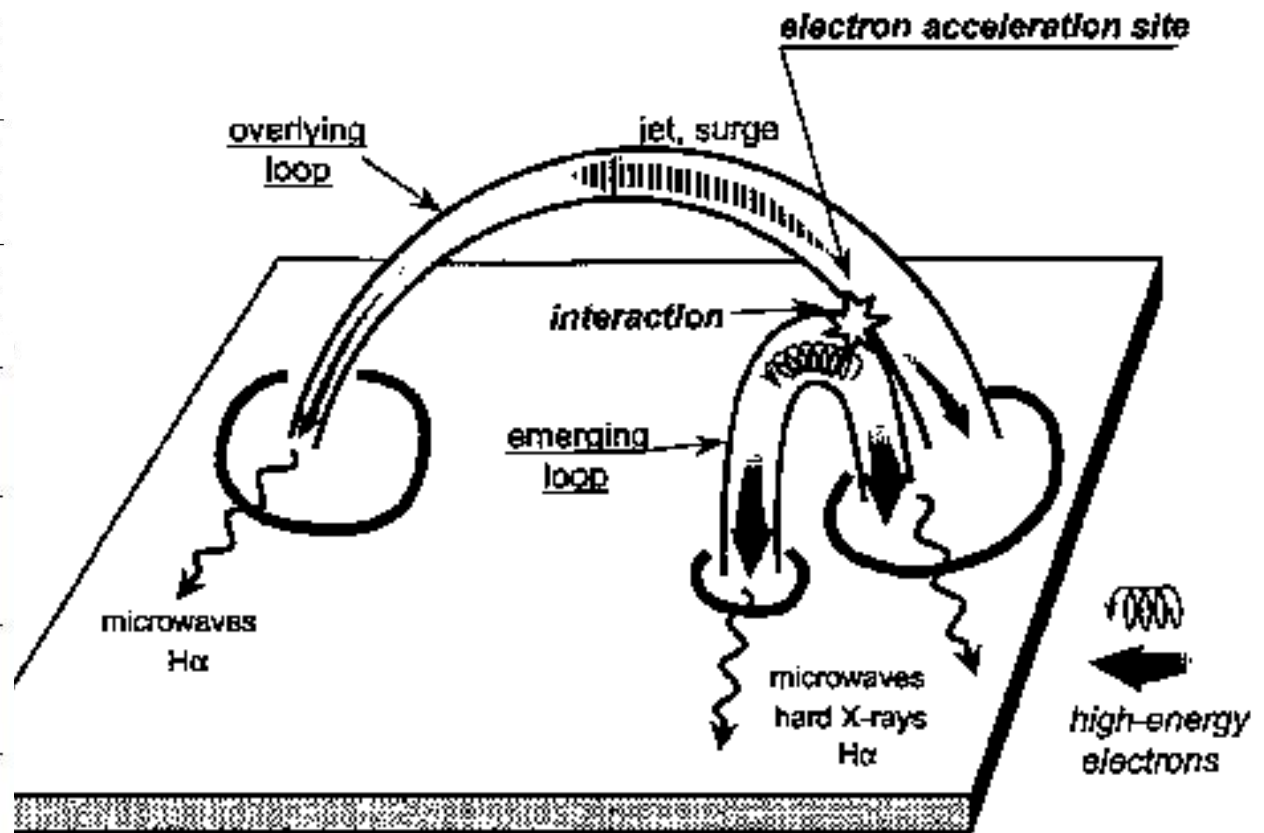
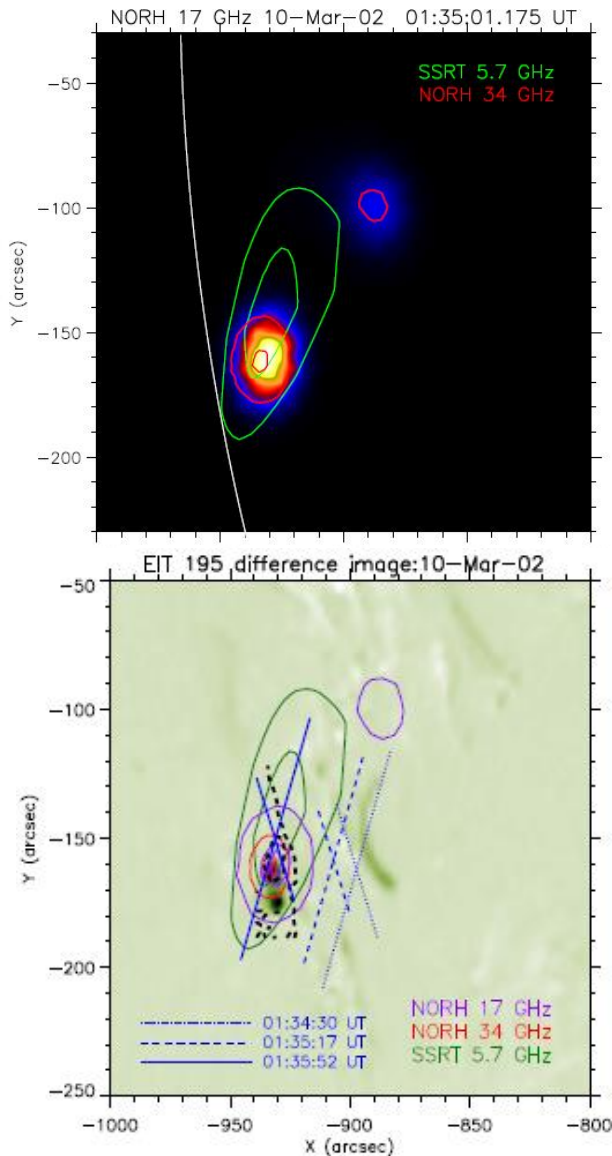
$$EM \sim 3 \cdot 10^{48} \text{ cm}^{-3}$$

$$A(> 50\text{G}) \approx 4.77 \cdot 10^{19} \text{ cm}^2$$



Nonthermal Model of This CF

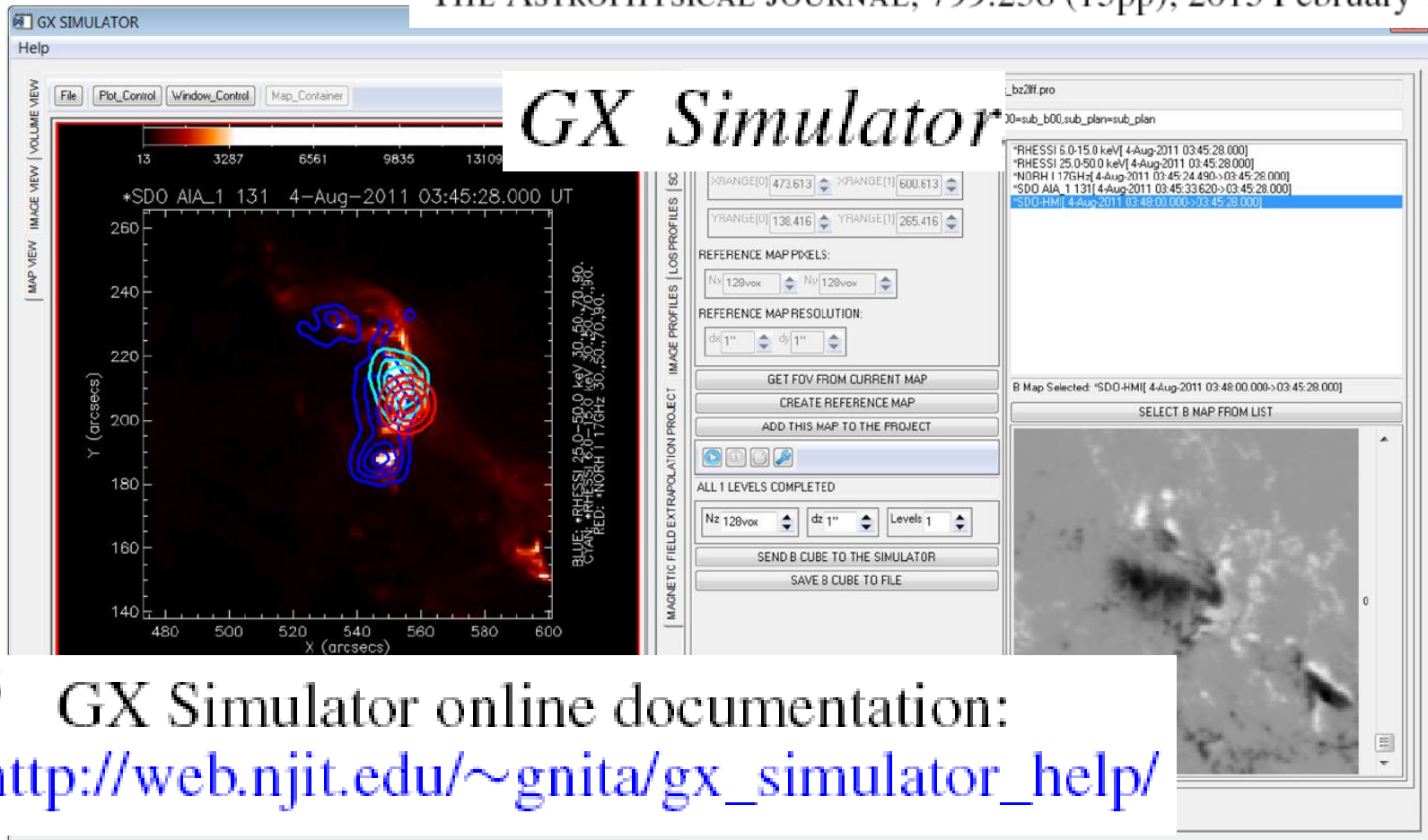
Hanaoka's model of a solar flare that occurred due to interaction between two magnetic loops



THREE-DIMENSIONAL RADIO AND X-RAY MODELING AND DATA ANALYSIS SOFTWARE: REVEALING FLARE COMPLEXITY

GELU M. NITA¹, GREGORY D. FLEISHMAN^{1,2}, ALEXEY A. KUZNETSOV³, EDUARD P. KONTAR⁴, AND DALE E. GARY¹

THE ASTROPHYSICAL JOURNAL, 799:236 (15pp), 2015 February 1

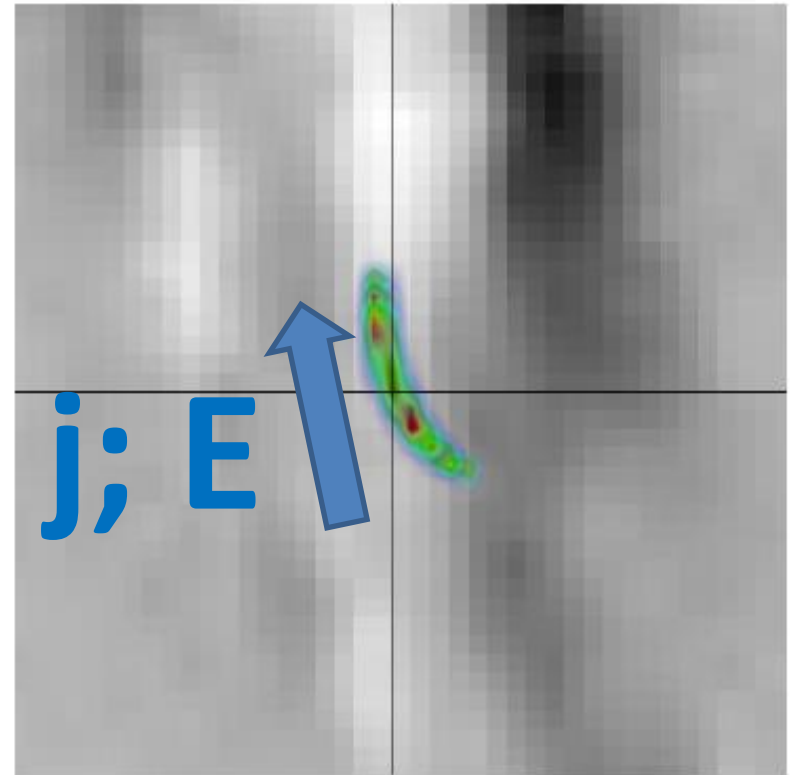
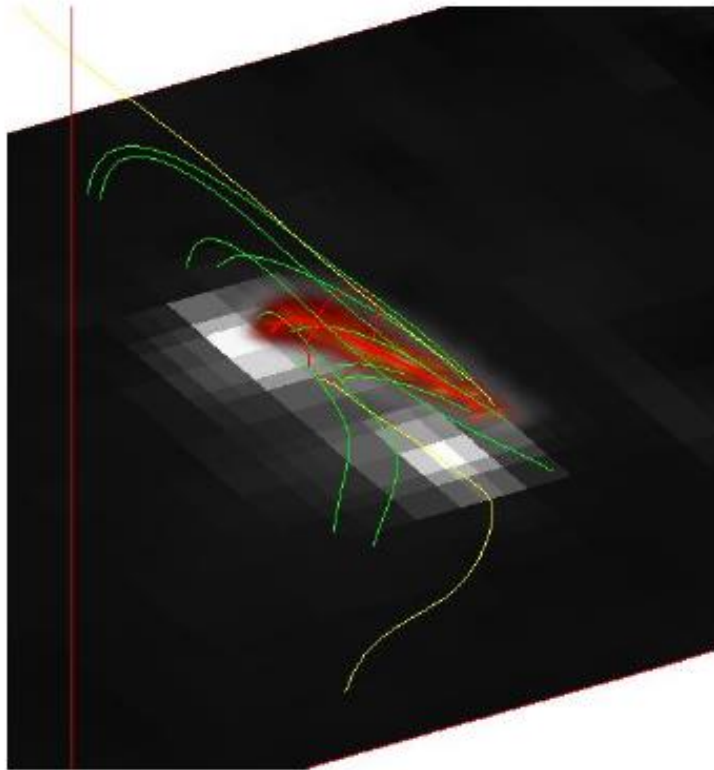


3D Modeling

linear force-free field ($\nabla \times \mathbf{B} = \alpha \mathbf{B}$ with a constant α , LFFF) extrapolation

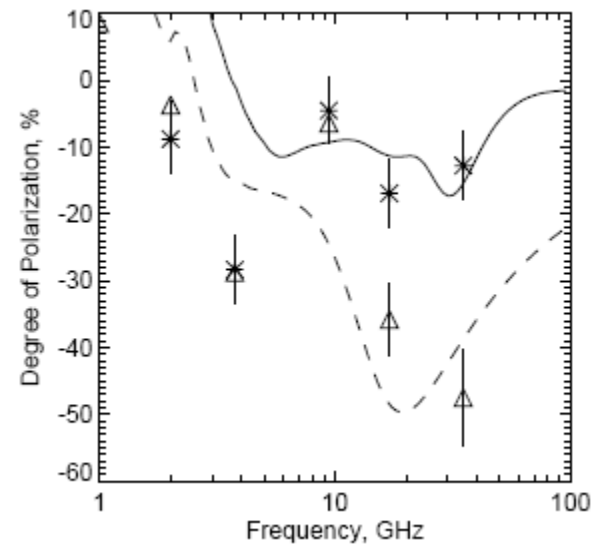
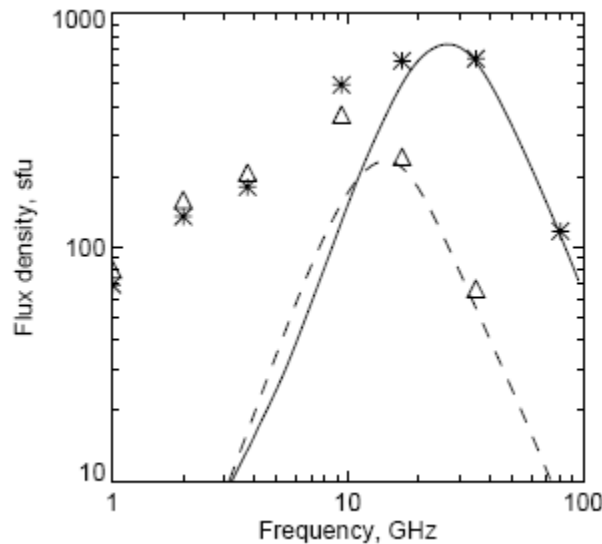
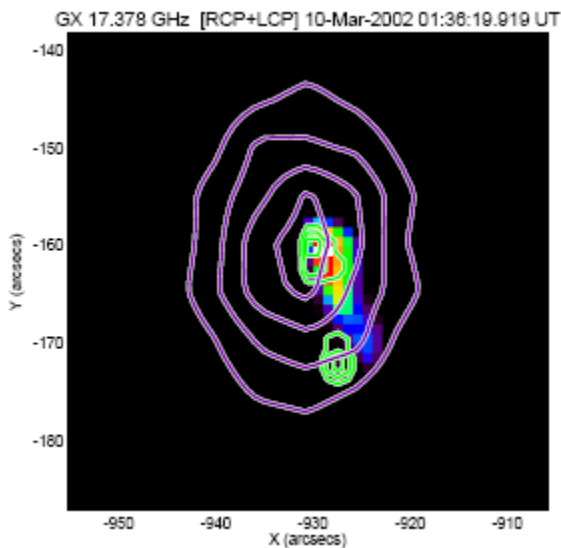
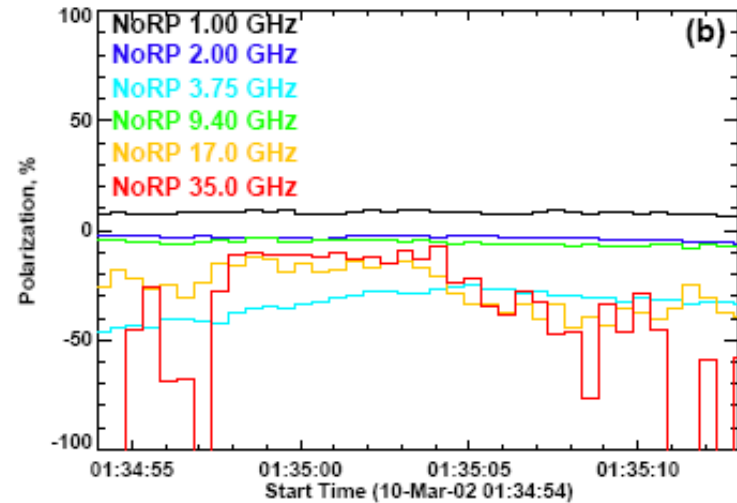
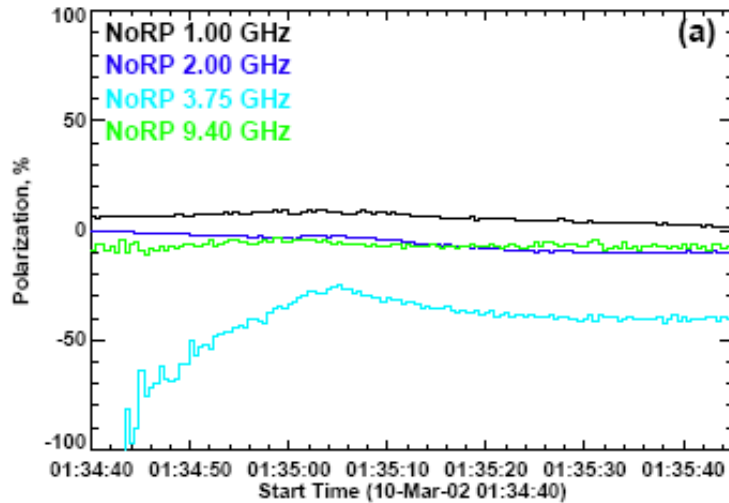
1. If the implied small and big loops can be reproduced in LFFF extrapolated data cubes and what α are needed for that?
2. Is it possible to populate the small loop with a distribution of fast electrons, which is consistent with the HXR data and, at the same time, capable of reproducing the high-frequency microwave spectrum?
3. Is it possible to populate the big loop with a distribution of fast electrons consistent with the HXR data to reproduce the low-frequency microwave spectrum?
4. Could the entire spectrum be reproduced by the two-loop model?
5. Is it possible to get the LCP polarization from both 17 GHz sources?
6. Is it possible to get the a very high degree of LCP polarization from the north 17 GHz source?
7. Could the entire polarization spectrum be reproduced by the two-loop model?

3D Modeling: Small Loop



$$\alpha \approx -1.75 \times 10^{-9} \text{ cm}^{-1}$$

High-frequency Radio Emission



The Best Fit

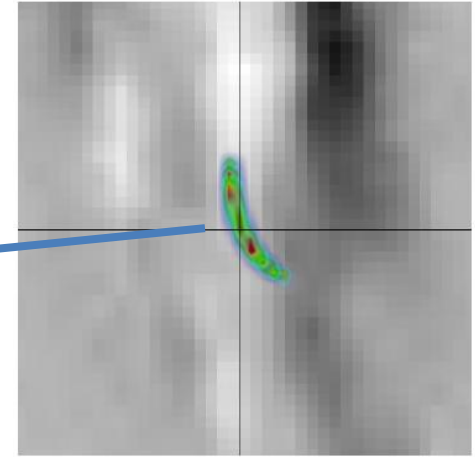
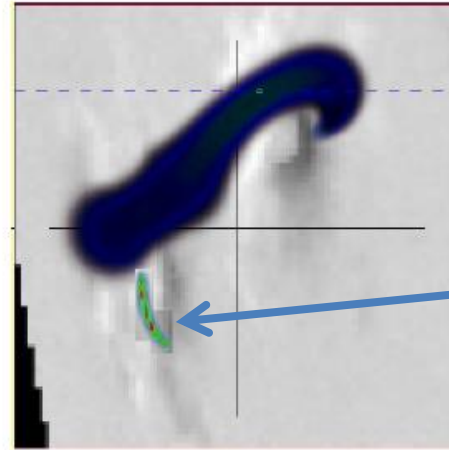
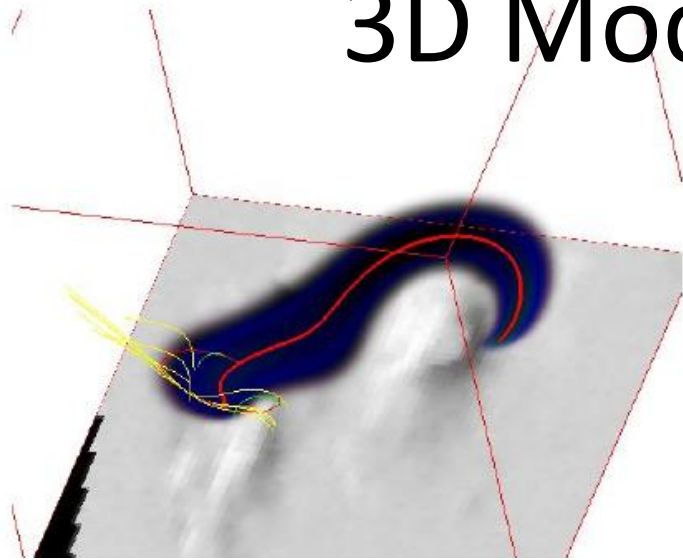
$$\delta_{r,1} = 2.5,$$
$$\delta_{r,2} = 3.5$$

The best fit is obtained for the number density of the fast electrons $n_r = 5.2 \times 10^8 \text{ cm}^{-3}$ (this is the peak value of the spatially nonuniform electron distribution) that corresponds to the total number of fast electrons at the source $N_{r,\text{tot}} \approx 1.35 \times 10^{34}$. Note, that the electron acceleration rate determined from the X-ray fit is about 1.2×10^{35} electron/s, which implies that the electron escape time τ_{esc} from the loop is roughly 0.1 s, which is three times larger than the time of flight ($L_{\text{small}}/c \sim 30$ ms) estimated for our loop length $L_{\text{small}} \sim 9 \times 10^8$ cm. Given the electron distribution is found to be beamed along the field lines, while the mirror ratio in this loop is small, ~ 2 , a more reasonable estimate for the escape time would be within 30 ms; this upper limit for the escape time is also implied by absence of any measurable (within 0.1 s time resolution) delay between the 35 GHz light curve and HXR light curves. Our two-loop model offers a natural solution for this discrepancy: with the numbers above we conclude that in fact the acceleration rate is roughly two-three times larger than the that derived from the HXR fit, but the remaining ($\sim 50 - 70\%$ of) accelerated electrons escape to the second, big loop, rather than precipitate to the small loop footpoints; thus, they do not contribute to the HXR emission.

The Best Fit

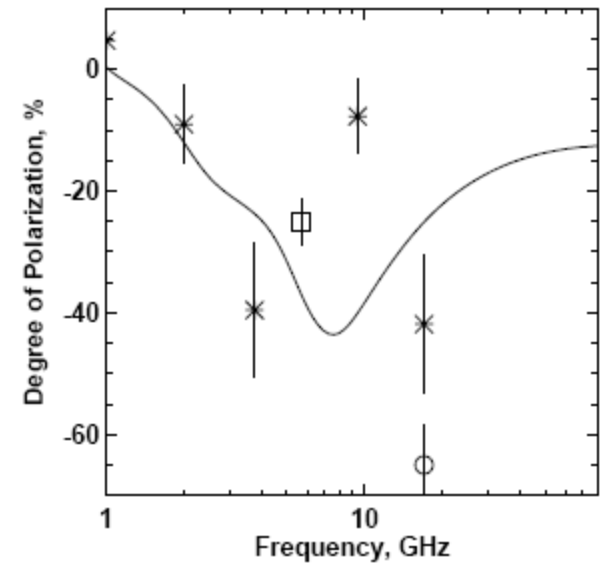
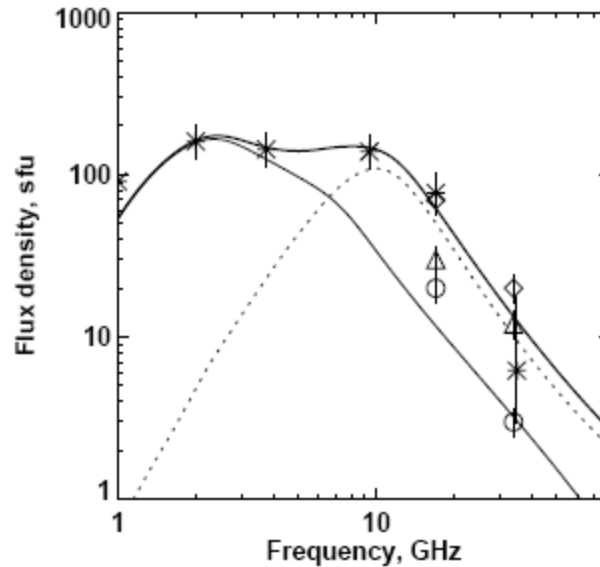
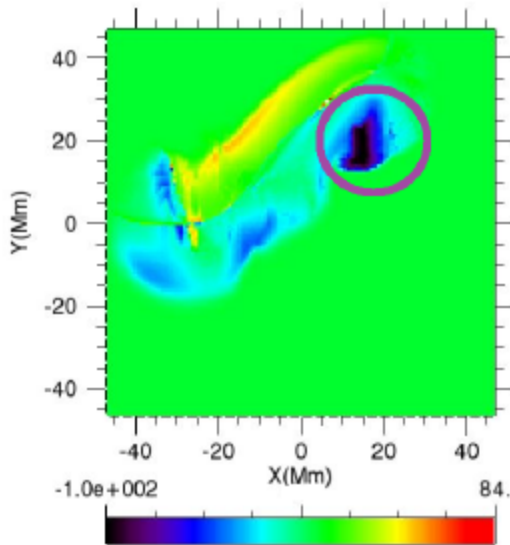
For spectral modeling of the big loop contribution we select the time 01:35:24.500 UT at the decay phase—rather close to the end of the prominent spectral evolution, where emission from the big loop presumably dominates the microwave spectrum. We get a reasonably good spectral match at low frequencies if we populate this magnetic loop with fast electron distribution within the energy range starting from the same $E_{\min} = 10$ keV in agreement with both HXR data and the small loop model to $E_{\max} = 5$ MeV,¹² and the number density $n_r = 1.6 \times 10^7$ cm⁻³ totaling in $N_{r,\text{tot}} \approx 5.7 \times 10^{34}$ electrons slightly concentrating towards the looptop, as expected due to particle trapping effect in the magnetic loops (Melnikov et al. 2002). The angular distribution is expected to have a loss-cone shape with the loss-cone angle $\theta_{\text{lc}} = 30^\circ$ in the top of the loop in agreement with the mirror ratio of four, but the isotropic distribution was found to give the same results, so we give here the numbers relevant to the isotropic model. The thermal plasma density at the central field line of the big loop is adopted to be $n_0 = 5 \times 10^9$ cm⁻³. This model offers a very good match for the low-frequency part of the total power spectrum and also reproduces the correct level of the spatially resolved data from the northern NoRH source at 17 GHz and 34 GHz, although the flux density of the northern source at 17 GHz is slightly underestimated. Similarly, the model slightly underestimates the flux density at 1 GHz, which indicates that the real source has a slightly stronger nonuniformity than the model one (cf. 3D models in Kuznetsov et al. 2011).

3D Modeling: Big Loop



$$\alpha \approx 1.16 \times 10^{-9} \text{ cm}^{-1}$$

[R-L]/[R+L][%] @ 17.4 GHz



Main Results

The data analysis and 3D modeling performed above in the paper suggest that all remarkable properties of this event can be quantitatively understood within a model involving energy release due to interaction of two non-potential magnetic flux tubes—one small and one big with different twists ($\alpha \approx -1.75 \times 10^{-9} \text{ cm}^{-1}$ and $\alpha \approx 1.16 \times 10^{-9} \text{ cm}^{-1}$, respectively). Electrons are accelerated due to interaction (magnetic reconnection) between these two loops and then divided in roughly equal numbers between these two loops. The electrons injected into the small loop has a beam-like distribution directed towards the southern EUV kernel, so most of them immediately precipitate into the southern footpoint of the small loop and produce the HXR emission there. On the fly, they interact with the magnetic field of the loop, which is reasonably strong in the small loop, varying from $B \sim 600 \text{ G}$ at the looptop up to $B \sim 1200 \text{ G}$ at the footpoints, to produce the high-frequency microwave emission as observed. The total number of fast electrons, $N_{\text{r,tot}} \approx 1.35 \times 10^{34}$, needed to match the high-frequency part of the microwave spectrum at the peak time requires a roughly double acceleration rate as compared with that derived from the HXR thick-target model fit, $\sim 1.2 \times 10^{35} \text{ electron/s}$.

Main Results

The missing electrons, those not seen via HXR emission, must have escaped to the big loop and be trapped there. To confirm this quantitatively, we note that at the decay phase time frame 01:35:24.500 UT, which we analyzed in great detail to validate the model, the total number of the trapped fast electron was found to be $N_{r,tot} \approx 5.7 \times 10^{34}$ to match the microwave spectrum. This implies that at the peak time of the gradual microwave light curves (01:35:05 UT), when the flux density at 3.75 GHz is twice bigger than at 01:35:24.500 UT, the number of the nonthermal electrons in the big loop must have been a factor of two larger, $N_{r,tot} \approx 1.2 \times 10^{35}$. This peak number of the fast electrons accumulated in the big loop is to be compared with the corresponding electron injection into the big loop. If we assume that the electron injection rate into the big loop is equivalent to the electron loss rate derived from the HXR thick-target spectral fit, the total number of electrons injected into the big loop would be $N_{inj} \sim 6 \times 10^{35}$ electrons over the impulsive phase of the flare; which, taken at the face value, is roughly five times larger than needed to supply the observed microwave emission from the big loop. Given that the number of the nonthermal electrons in the big loop is determined using a poorly defined low-energy spectral index and low-energy cut-off in the big loop, we conclude that the obtained electrons numbers are consistent with each other and so having a half of the accelerated electrons or slightly less to escape towards the big loop is sufficient to supply it with the required number of the fast electrons needed to match the low-frequency part of the microwave spectrum.

Conclusions

In this study we identified a new “cold” solar flare whose properties and physical model are substantially different from the cold flares reported so far (Bastian et al. 2007; Fleishman et al. 2011; Masuda et al. 2013). In contrast to the known cold flares, which consisted of one main loop, the described here 2002-03-10 cold flare is a vivid example of interaction between two loops. The first of them, a small one, is responsible for the impulsive flare component, while the bigger one is responsible for a more gradual nonthermal emission. Interestingly, the electrons accelerated in the event divided roughly evenly between these two loops, which made both loops comparably important in driving the thermal response in this event. For this reason the GOES flare was substantially delayed relative to the impulsive peak in apparent contradiction with the conventional Neupert effect. However, taking into account in situ coronal losses of the fast electron component trapped in the big loop, we obtained a scenario fully consistent with the plasma heating by the accelerated electrons—in a remarkable agreement with spirit of the Neupert effect. The developed model is in quantitative agreement with observations, including microwave imaging and polarization, and naturally identifies the cause of the suppressed chromospheric evaporation that is needed to interpret the unusually weak GOES response in this flare.